SAND2011-2625C

Integrated Chip-Scale THz Technology

Michael C. Wanke[a], Mark Lee[a,b], Christopher D. Nordquist[a], Michael J. Cich[a], Melissa Cavaliere, Adam M. Rowen[a], James R. Gillen[a], Christian L. Arrington[a], Albert D. Grine[c], Charles T. Fuller[a], John L. Reno[a]

[a]Sandia National Laboratories, Albuquerque, NM, USA;
[b]Now at University of Texas, Dallas, TX, USA;
[c]LMATA Government Services, Albuquerque, NM, USA

ABSTRACT

The quantum cascade laser (QCL) is currently the only solid-state source of coherent THz radiation capable of delivering more than 1 mW of average power at frequencies above $\sim$ 2 THz. This power level combined with very good intrinsic frequency definition characteristics make QCLs an extremely appealing solid-state solution as compact sources for THz applications. I will present results on integrating QCLs with passive rectangular waveguides for guiding and controlling the radiation emitted by the QCLs and on the performance of a THz integrated circuit combining a THz QCL with a Schottky diode mixer to form a heterodyne receiver/transceiver.

Keywords: Quantum Cascade Laser, Terahertz, Transceivers, Heterodyne Receiver, Rectangular Waveguides

1. INTRODUCTION

THz quantum cascade lasers have achieved the level of performance[1–4] required to begin exploring their use in applications.[5–7] In an application, however, the THz laser is only one component of a larger system and coupling of the THz QCL to the rest of the system components including optics, targets, or detectors needs to be controlled for best performance.

One application that is particularly of interest is using THz QCLs as local oscillators for heterodyne receivers, especially for astrophysical instruments. Typically the QCL is used as a standalone device, and the output of the laser is collected and refocused quasi-optically onto separate detectors such as hot-electron bolometers[8,9] or Schottky diodes.[10,11] Due to the size of the wavelength, the quasi-optical components are significantly larger than either the typical QCL or mixer, resulting in a system much larger than the individual components. In addition, the beam pattern from edge emitting QCLs (in particular from QCLs employing metal-metal waveguides) is not a simple Gaussian which can lead to coupling issues.

The microelectronic nature of THz QCLs enables one to integrate them with other components on the same chip to make THz photonic integrated circuits (IC), which could significantly reduce system sizes. While integration should lead to higher functionality devices as it did in microwave and infrared photonics, so far integration of THz QCLs has mostly been limited to adding passive microwave components to improve emitted beampatterns.[12–15]

Over the past few years, we have pursued two paths to making THz integrated circuits: (a) integrating metal-metal waveguided QCLs with on-chip rectangular waveguides and (b) integrating Schottky diodes directly into the core of an THz QCL. This paper reviews some of that previous work, presents some newer results and discusses future opportunities.

Further author information: (Send correspondence to Michael Wanke)
Michael Wanke: E-mail: mcwanke@sandia.gov, Telephone: 1 505 844 2532

2. QCL / RECTANGULAR WAVEGUIDE INTEGRATION

Integrating QCLs into rectangular waveguides has multiple potential benefits over quasi-optical coupling. Rectangular waveguides are widely used for moving low THz frequency signals around in a compact volume. The propagation and mode structure of THz radiation through rectangular waveguides is fairly well understood and many passive components can be fabricated to not only guide the light, but also to split or combine beams. The mode structure of the waveguide can be used to control the modes emitted by the laser. By connecting appropriate horns to the waveguides, the spatial beam pattern of THz radiation coupled out into free space can be significantly improved (especially for metal-metal QCLs) since the pattern will be defined by the horn rather than by the sub-wavelength aperture of the laser. This is advantageous for long distance beam propagation and for coupling to other devices where good mode control is important. Many available mixers are already embedded in rectangular waveguide blocks so by integrating a QCL into a compatible block, the QCLs could be mated with existing technology and infrastructure. By keeping the laser and diode as individual components linked via a waveguide, each component can still be optimized separately (as compared to our integrated transceivers described below). Even with the components in isolated rectangular waveguide blocks, they can more easily be assembled into a system that is more compact and robust than using quasi-optics.

Rather than follow the conventional approach of machining a rectangular waveguide into a metal block, placing a device in the proper location, and bolting it to another metal block, we lithographically defined and fabricated waveguides directly on semiconductor chips with THz QCLs already fabricated on the surface. The lithographic process has the advantages of being compatible with microelectronic fabrication, being able to make lots of waveguides in parallel, and improving the placement accuracy. In addition this process results in much lower surface roughness than traditional machining, which decreases the waveguide loss at THz QCL frequencies. Detailed descriptions of the fabrication steps and performance are described elsewhere.[14,16,17]

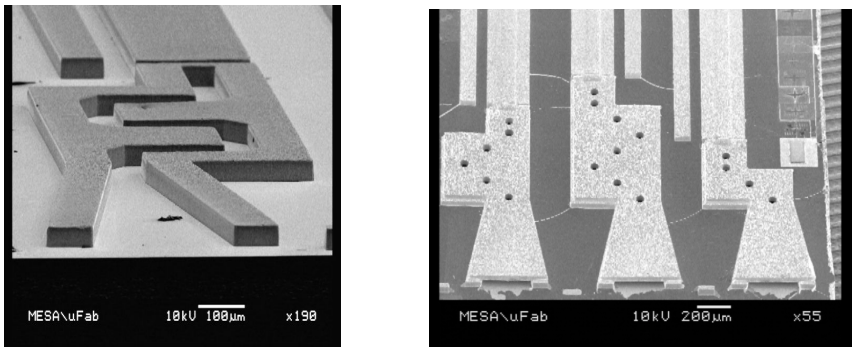

Figure 1.

The micromachined waveguide structures have a waveguide channel 75 μm wide by 37 μm tall, designed to operate single-mode at frequencies around 3 THz. Figure 1 shows a few typical waveguides. The left image shows just the sidewalls of a waveguide on a dummy wafer while the right image shows three completed waveguides integrated with 3 QCLs. The waveguides shown in these images all have H-plane bends. The L-I-V and spectra shown in Fig. 2 for the 6-bend waveguide demonstrate that the THz radiation can be steered and turned on the chip and coupled out to free space via a 2-dimensional horn flare. The radiation can also be coupled out vertically by putting an E-plane bend in the waveguide as shown in Fig. 3(a). In this case the waveguide terminates abruptly. This is not ideal for coupling out into free space, but the L-I-V shown in Fig. 3(b) demonstrates that we can still measure the THz emission. It may be easier to couple vertical emission openings to separately fabricated 3D horns which would provide a further improvement of the emitted beampattern over the 2D flared horns currently demonstrated.

Previous measurements of the THz propagation through non-integrated waveguides[17] yielded losses of 1.8, 1.6 and 1.3 dB/mm at 2.56, 2.84 and 3.11 THz respectively. These values are roughly twice what is predicted, which may be due to nonideal gold conductivity, surface roughness, photoresist residues on the waveguide walls, or residual Ti on the waveguide walls. Depending on the actual cause, further reduction of loss may be possible. Encouragingly, when normalized per wavelength, the measured losses of approximately 0.20, 0.16, and 0.12 dB/λ,

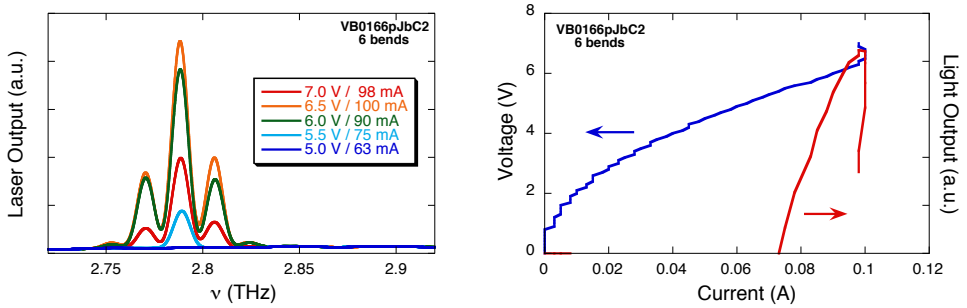

Figure 2. Spectra (left) and L-I-V (right) for the center waveguide shown in Fig. 1(b) with 6 H-plane bends.

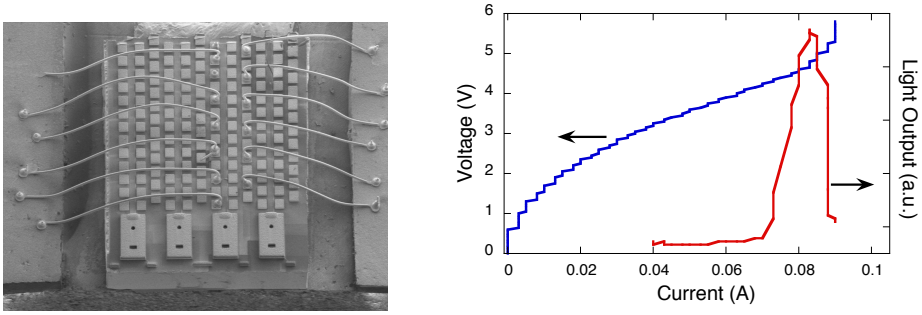

Figure 3. Picture and L-I-V of QCLs coupled to rectangular waveguides with E-plane bend and surface normal emission.

are of similar magnitude to previously reported measurements of 0.2 dB/λ at 100 GHz[18] and 0.6 dB/λ[19] at 300 GHz. For most envisioned uses of moving THz signals around on a chip, the distances should be fairly short and the measured loss values should not be a significant problem.

The beampatterns of bare, edge-coupled, metal-metal THz QCLs are rather complicated,[20] and this complexity can significantly reduce the amount of emitted power that can be harnessed for use in an application. Only one spatial mode can propagate in a (properly sized) rectangular waveguide, so the output of THz QCLs coupled into a rectangular waveguide will automatically be single mode. By flaring the waveguide into a horn structure to couple the radiation to free space, the effective aperture can be increased and the divergence of the emitted beam decreases. For our horns we only flared the horn on one axis. Therefore, although the rectangular waveguides are roughly 4 times taller than the height of the QCL facet, the horn openings along the vertical axis are still sub-wavelength so we still expect the beam to diverge rapidly along the vertical axis. The flared horn is multiple wavelengths wide horizontally, so we expect the divergence along the horizontal axis to be significantly less. Even with the large vertical divergence, the beam quality should still be better than that of a bare metal-metal edge coupled laser since the waveguide and horn should couple out a single spatial mode rather than the more complicated wire-laser emission pattern.[21]

We have made preliminary beampattern measurements on stand-alone waveguides (illuminated at the other end by a far-infrared molecular gas laser (FIRL)), and on a waveguide integrated with a QCL. A cartoon showing the measurement is shown in Fig. 4(a) (although in reality an off-axis paraboloid is used instead of a refractive lens). Since we are really using an off-axis paraboloid for the lens, the angles will be distorted somewhat, but the explanation of the corrections will not be presented here. The measured beampattern for the stand-alone waveguides is shown in Fig. 4(b), and as expected the beam diverges faster in the vertical direction although not as much as expected.

For the integrated QCL/waveguide sample, the device is in a cryostat and has an extra window between the horn and lens. The results from the QCL are shown in Fig. 5. Because of the orientation of the cold-finger in the cryostat, the sample is rotated 90 degrees compared to the empty waveguide orientation so the divergence should be higher along the horizontal axis. The measured beampattern for the QCL integrated waveguide shown in Fig. 5. Rather than seeing a single spot elongated along the horizontal axis, we observed a fairly tight spot

with a couple of fringes near the edge of the mirror. The high resolution image shows a lot of fringes. These are only preliminary measurements and future work is needed to explore the cause of the fringes and the differences observed between empty and integrated waveguides.

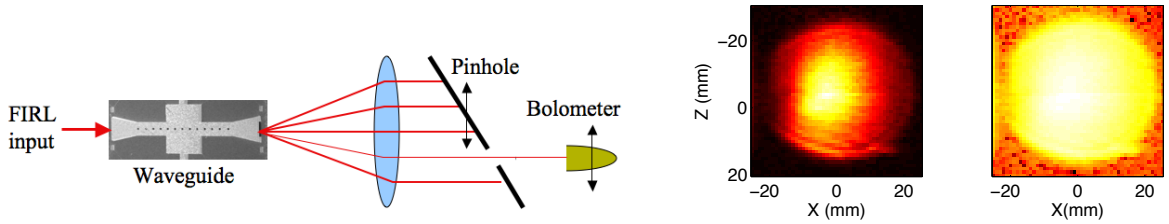

Figure 4. (a) Cartoon depicting the essential elements for measuring the beam pattern. The pinhole and bolometer move together. (b) Image of the beampattern as collected by the lens for a standalone waveguide driven by a molecular gas laser. The color scale for the left image is on a linear scale, while the right is logarithmic.

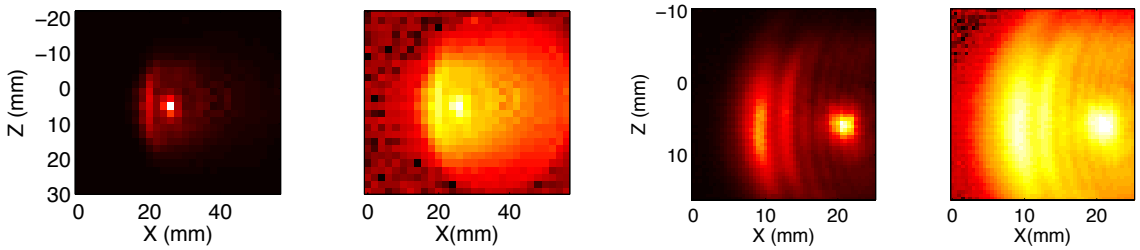

Figure 5. (a) Measured beampattern image of output from a waveguide integrated with a QCL (b) Higher-resolution image of the beampattern using a 1 mm diameter pinhole, showing probable interference effects from the cryostat window. The color scale for the left image is on a linear scale, the right is logarithmic.

Besides providing a way to improve the beam pattern of a metal-metal QCL, the integrated waveguide also allows engineering of the output coupling. Due to the extreme sub-wavelength aperture in the vertical direction, the typical facet reflectivity of the QCL is on the order of 95% which limits the output power. One way to improve the out-coupling is to add a Si lens to the facet,[22] however, this adds alignment complexity and has the potential to damage the laser facet. Fig. 11 in reference [14] shows that simply terminating the QCL facet into a rectangular waveguide should immediately increase the outcoupling up to 40%, in a simple manufacturable process.

In fact, the effective facet reflectivity can be engineered to a desired value by altering the interface between the QCL and the waveguide. If the impedance has a large mismatch, the reflectivity will be high and little power will exit the laser. While this will lead to low output powers, it should also lower the threshold current and could raise the operation temperature. If there is no mismatch we effectively achieve an anti-reflection coating so that there will be no feedback and lasing will cease. In this case, an additional feedback mechanism, such as a distributed feedback grating or an external cavity, would be needed to achieve lasing. A possible advantage of using an external grating for feedback would be the ability to tune the laser frequency over a broader range. For intermediate values of the mismatch, we should be able to go between these extremes to find the optimal power output or the optimal efficiency.

A simple approach for controlling the reflectivity of the QCL/ waveguide interface involves tapering the facet of the QCL to a point as depicted in Fig. 6(a), rather than having a rectangular termination. To explore this concept, we simulated the coupling between the QCL and the waveguide as a function of the taper length. In our simulations, the top contact metal does not extend into the waveguide with the laser material. While in reality, the QCL material will have losses, we modeled this tapered section as undoped GaAs to simplify our simulations. Fig. 6(b) shows the expansion of the E-field predicted from an HFSS simulation. The field spot size gradually grows from the confined microstrip mode of the laser to the large mode of the rectangular waveguide. This simple design has the distinct appealing advantage of requiring only a single processing step to define the waveguide transition region.

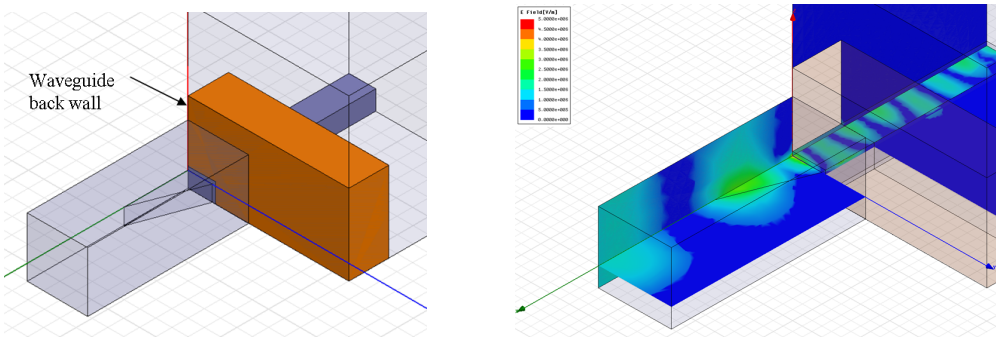

Figure 6. (a) Half-model of a QCL-RWG interface showing dielectric material extension into the waveguide. Only half of the model is shown due to symmetry about the center of the waveguide. (b) E-field expansion in the tapered QCL-RWG transition.

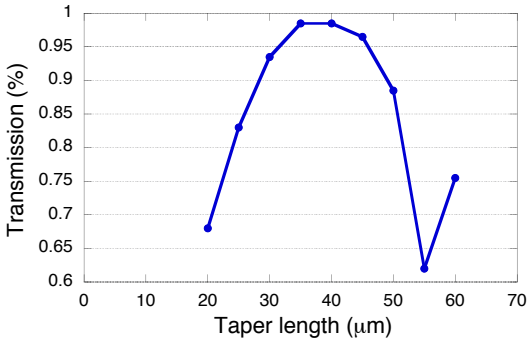

Figure 7. Transmission as a function of taper length for the tapered transition design.

The simulated transmission as a function of the length of the dielectric extension into the waveguide is shown in Fig. 7. As shown, the effective transmission of the QCL/waveguide interface can be tuned over a fairly wide range. If we shrink the taper back to zero length we approach the 40% predicted previously.[23] The maximum calculated transmission ($\sim 98\%$ for the lengths explored) occurs at a length of 40 μm, which is approximately $\lambda/2$ in the dielectric-loaded waveguide. The high near-unity transmission at the peak suggests this may be a good possibility for making an effective antireflection "coating" on THz QCLs. WIth further integration to couple the rectangular waveguides to fully 3 dimensional horns, it would even be possible to use metal-metal QCLs in external cavities since the waveguide and horn could recollect the large mode size from the external optics and couple it back into the subwavelength aperture of the laser.

Another possible opportunity is to connect a horn-coupled rectangular waveguide to both ends of a THz QCL. Since the gain bandwidth of a THz QCL can be very broad, with both QCL/waveguide interfaces impedance matched the QCL could act as a broadband amplifier. Others have demonstrated using a QCL as an amplifier for ultrashort laser pulses.[24] Since the rectangular waveguide has significant dispersion and the short pulses have a broad bandwidth rectangular waveguides are not be ideal for this application, but they would work well with cw sources.

3. INTEGRATED THZ TRANSCEIVER

By integrating a Schottky diode into the core of a THz QCL we created a monolithically integrated THz transceiver-on-a-chip.[25] This THz photonic IC performs all the basic receiver functions performed by discrete component THz photonic systems but at a small fraction of the size and in a robust platform scalable to semiconductor fabrication production. Not only is the size reduced, but by integrating the mixer directly into the laser core, we can reduce coupling losses between the laser and the mixer. Additionally, since the mixer is permanently fixed to the laser itself alignment is fixed, making the device extremely robust. This design also has the promise

of reducing the laser power requirement by a couple of orders of magnitude, resulting from the improved coupling combined with tapping into the internal laser fields which are always higher than the fields emitted by the laser.

In a typical THz transceiver, a local oscillator source is coupled to a separate mixer via an optical or waveguided path. By monolithically integrating a Schottky diode into a small opening in the top contact metallization of a typical THz quantum cascade laser (Fig. 8(a)), we eliminate the quasi-optical components. Since cladding layers are not used in the lasers, the internal lasing field has a strong overlap with the semiconductor metal interface. Therefore, a portion of the internal propagating field inside the QCL cavity is coupled to the diode which is created at the metal/semiconductor interface, eliminating the propagation path between the source and mixer. Further details on the construction and operation of the transceiver are provided elsewhere.[23,25]

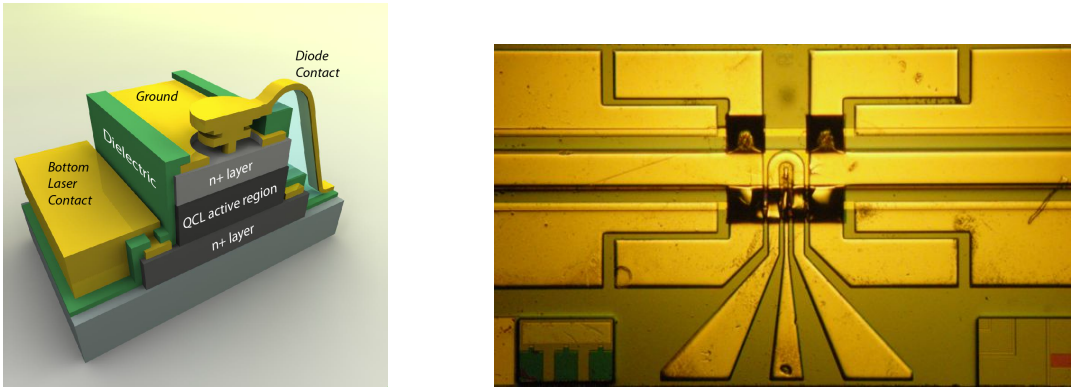

Figure 8. (a) Cartoon of the original conception for integrating a Schottky diode mixer with a QCL. (b) an optical picture of the central part of a fabricated transceiver. The outermost contacts provide the laser bias. The middle contacts provide the ground to the top of the laser stripe, and the inverted-V-shaped contacts are the coplanar waveguide connecting the diode in the center of the image.

The non-linearity of the diode current-voltage (I-V) characteristic serves to rectify and mix the THz fields inside the laser to provide d.c. and RF responses. These THz fields inside the laser can be self-generated modes of the laser itself or externally generated fields coupled into the laser through one of the laser facets. Figure 9 shows a typical RF spectrum produced by the diode over the 26 GHz bandwidth of the measurement. In this figure, one can identify the beat frequency of the nearest-neighbor Fabry-Perot modes of the laser (∼13 GHz), the beat frequency of the next-nearest neighbor Fabry-Perot modes (∼26 GHz), the beat frequencies between four Fabry-Perot modes of the transceiver and a separate single mode DFB THz QCL injected into one facet of the transceiver (∼4, 9, 17 and 22 GHz), and a couple of extra peaks due to electrical pick-up from other lab equipment. The four beat frequencies between the transceiver and the external laser correspond to peaks δ, $13-\delta$, $13+\delta$, and $26-\delta$, as depicted in figure 3 in reference[25].

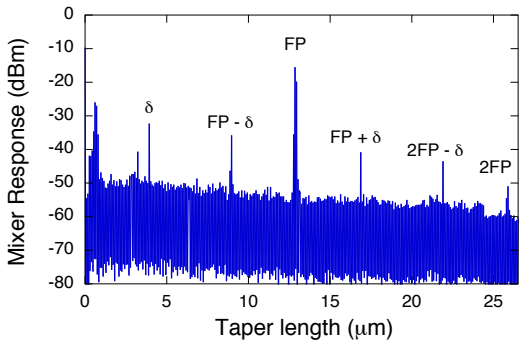

Figure 9. 26 GHz bandwidth RF spectrum produced by the integrated diode, when the transceiver laser is running on multiple Fabry-Perot modes, and a separate single mode THz QCL is injected into one transceiver facet.

We have shown elsewhere that this transceiver performs all the basic receiver functions performed by discrete component THz photonic systems (e.g., transmission of a coherent carrier, heterodyne reception of an external signal, frequency and phase locking, and tuning). These can be used not only to measure externally incident signals, but can be used to monitor the performance and behavior of the transceiver QCL as well.

One characteristic of the QCL that we have shown previously[23] is that the difference frequency between the transceiver's multiple Fabry-Perot laser modes is sensitive to feedback. By changing the distance of a mirror that retroreflects some or all of the laser emission back into the transceiver, the difference frequency (and its amplitude) will oscillate as a function of the mirror distance with a period of $\lambda/2$ (see Fig. 10). The shape and the magnitude of the oscillation depend on the strength of the feedback, the distance to the mirror, the laser current, and the laser temperature, but the general oscillating behavior is independent of these parameters. When the mirror is scanned through only a few wavelengths the oscillation is nearly periodic, but for longer scans, the shape of the oscillations can be quite different from one end of the scan to the other.

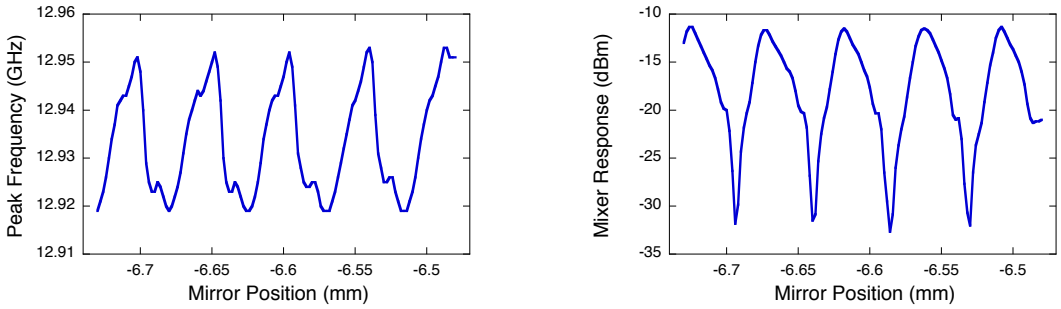

Figure 10. (a) Frequency difference between Fabry-Perot modes and (b) the amplitude of the mixer response in a transceiver as a function the distance to a retroreflecting mirror.

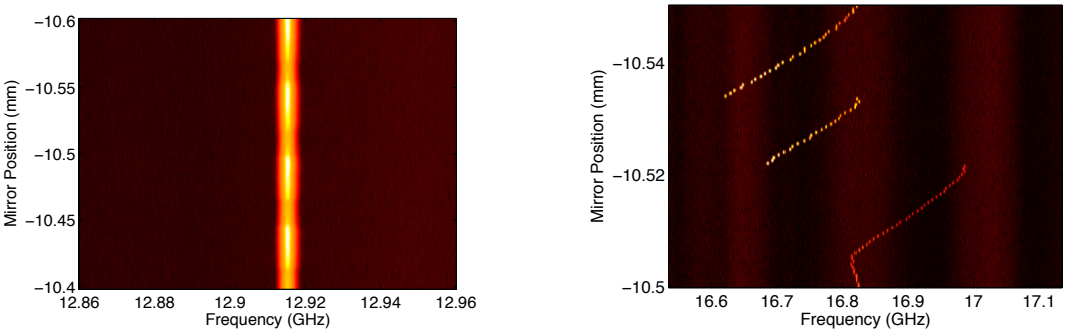

Figure 11. Retroreflector mirror distance dependence of the (a) difference frequency of the internal Fabry-Perot modes and (b) the difference frequency between one internal FP mode and a separate, externally injected, distributed feedback, THz QCL, when the internal modes of the transceiver are phase-locked.

As described in the supplementary material in reference [25] the beat frequency between the Fabry-Perot modes can be phase-locked to within 1 Hz. This phase lock is robust enough that it is maintained in the presence of strong feedback, even when the retroreflecting mirror is scanned. While the beat frequency remains constant as the mirror moves, the amplitude of the beat signal fluctuates periodically with a period of $\lambda/2$ (see Fig. 11(a)). By simultaneously injecting the emission of a separate, single-mode QCL into the transceiver we can also extract how the THz frequency of one or more modes of the laser reacts to the retroreflector distance. Fig. 11(b) shows that even though the beat frequency between the QCL modes is fixed, the measured absolute frequency of one (and hence the absolute frequency of all) of the modes changes by nearly 400 MHz and exhibits sudden jumps as the mirror distance changes by $\lambda/2$. Since we do not have an optical isolator at 3 THz, the separate THz QCL may experience some feedback as well. Since the measurement displayed in Fig. 11(b) only determines the difference frequency between the two lasers, there is the possibility that all of the measured frequency change was

not due to transceiver frequency changing and that DFB frequency might have been pulled as well. Additional measurements showing that the modes of the transceiver do in fact change even when the modes are phase-locked will be published elsewhere.

Figure 12. (a) 2D plot of the difference frequency between the Fabry-Perot modes of the transceiver when the emitted radiation is focused to a spot and reflected off a Georgia quarter which is scanned in the focal plane.

We can harness the fact that the beat frequency of the laser depends on the distance to a retroreflecting object to look at surface topology of a non-planar surface. Since the frequency of the beat frequency is not unique to a certain distance (as shown in Fig. 10(a)), this is better suited to surfaces with height variations on the surface less than $\lambda/2$. However, as a preliminary example we collimated the output of the transceiver and refocused it onto the surface of a quarter. The difference frequency of the Fabry-Perot modes of the transceiver as the quarter is raster scanned across the focal spot of the beam emitted by the transceiver, along with a visual image of the quarter, are shown in Fig. 12. Instead of scanning the whole quarter at once, the quarter was imaged in sections and the sections reassembled. The slight color difference between sections is a result of slight differences in spectral ranges. Darker shades are lower in frequency and the range is about 100 MHz. The image is clearly identifiable and features comparable to the wavelength (100 μm) can be seen.

One of the issues with the current integrated transceiver is relatively low coupling of external radiation into the laser. We showed previously[23] that we could not observe coupling of external radiation to the diode via a connected simple dipole antenna, but we were able to couple radiation in through the facets. Since the facet is relatively small (especially for metal-metal THz QCLs) and the beam pattern is non-gaussian, the efficiency of coupling external radiation into the laser through the facet is quite low. The power coupled into the waveguide could be significantly improved by combining both of the integration schemes discussed here and integrating a waveguide and horn antenna onto the facet of the QCL.

4. SUMMARY

We've been working towards creating monolithically-integrated, chip-scale, THz technology centered on quantum cascade lasers as active THz sources. We have demonstrated direct on-chip mating of lithographically defined rectangular waveguides to THz QCLs and have demonstrated that the THz power can be guided around on chip with low enough loss to be practical for coupling on-chip devices. Furthermore, we integrated a Schottky diode mixer directly into the core of a THz QCL to create an integrated THz transceiver-on-a-chip. This THz photonic IC performs all the basic receiver functions performed by discrete component THz photonic systems (e.g., transmission of a coherent carrier, heterodyne reception of an external signal, frequency and phase locking and tuning), but at a small fraction of the size and in a robust platform scalable to semiconductor fabrication production. These two steps represent two possible building blocks which could be used to build higher functionality THz integrated circuits in the future.

ACKNOWLEDGMENTS

This work was funded by the laboratory directed research and development (LDRD) program office at Sandia National Laboratories. Sandia is a multiprogram laboratory operated by Sandia Corporation, a Lockheed Martin

Company, for the United States Department of Energy's National Nuclear Security Administration under contract DE-AC04-94AL85000.

REFERENCES

[1] Williams, B., Kumar, S., Hu, Q., and Reno, J., "High-power terahertz quantum-cascade lasers," Electron Lett **42**, 89–91 (Jan 2006).

[2] Walther, C., Fischer, M., Scalari, G., Terazzi, R., Hoyler, N., and Faist, J., "Quantum cascade lasers operating from 1.2 to 1.6 thz," Appl Phys Lett **91**, 131122 (Jan 2007).

[3] Kumar, S., Hu, Q., and Reno, J. L., "186 k operation of terahertz quantum-cascade lasers based on a diagonal design," Appl Phys Lett **94**, 131105 (Jan 2009).

[4] Williams, B. S., "Terahertz quantum-cascade lasers," Nat Photonics **1**, 517–525 (Jan 2007).

[5] Richter, H., Greiner-Baer, M., Pavlov, S. G., Semenov, A. D., Wienold, M., Schrottke, L., Giehler, M., Hey, R., Grahn, H. T., and Huebers, H.-W., "A compact, continuous-wave terahertz source based on a quantum-cascade laser and a miniature cryocooler," Opt Express **18**, 10177–10187 (Jan 2010).

[6] Barbieri, S., Alton, J., Baker, C., Lo, T., Beere, H., and Ritchie, D., "Imaging with thz quantum cascade lasers using a schottky diode mixer," Opt Express **13**, 6497–6503 (Jan 2005).

[7] Lee, A. W. M., Williams, B. S., Kumar, S., Hu, Q., and Reno, J. L., "Real-time imaging using a 4.3-thz quantum cascade laser and a 320 x 240 microbolometer focal-plane array," Ieee Photonic Tech Lett **18**, 1415–1417 (Jan 2006).

[8] Gao, J., Hovenier, J., Yang, Z., Baselmans, J., Baryshev, A., Hajenius, M., Klapwijk, T., Adam, A., Klaassen, T., Williams, B., Kumar, S., Hu, Q., and Reno, J., "Terahertz heterodyne receiver based on a quantum cascade laser and a superconducting bolometer," Appl Phys Lett **86**, 244104 (Jan 2005).

[9] Hubers, H., Pavlov, S., Semenov, A., Kohler, R., Mahler, L., Tredicucci, A., Beere, H., Ritchie, D., and Linfield, E., "Terahertz quantum cascade laser as local oscillator in a heterodyne receiver," Opt Express **13**, 5890–5896 (Jan 2005).

[10] Lee, M., Wanke, M. C., Lerttamrab, M., Young, E. W., Grine, A. D., Reno, J. L., Siegel, P. H., and Dengler, R. J., "Heterodyne mixing of terahertz quantum cascade lasers using a planar schottky diode," Ieee J Sel Top Quant **14**, 370–373 (Jan 2008).

[11] Barbieri, S., Alton, J., Beere, H., Linfield, E., Ritchie, D., Withington, S., Scalari, G., Ajili, L., and Faist, J., "Heterodyne mixing of two far-infrared quantum cascade lasers by use of a point-contact schottky diode," Opt Lett **29**, 1632–1634 (Jan 2004).

[12] Lloyd-Hughes, J., Scalari, G., van Kolck, A., Fischer, M., Beck, M., and Faist, J., "Coupling terahertz radiation between sub-wavelength metal-metal waveguides and free space using monolithically integrated horn antennae," Opt Express **17**, 18387–18393 (Jan 2009).

[13] Maineult, W., Gellie, P., Andronico, A., Filloux, P., Leo, G., Sirtori, C., Barbieri, S., Peytavit, E., Akalin, T., Lampin, J.-F., Beere, H. E., and Ritchie, D. A., "Metal-metal terahertz quantum cascade laser with micro-transverse-electromagnetic-horn antenna," Appl Phys Lett **93**, 183508 (Jan 2008).

[14] Wanke, M. C., Nordquist, C. D., Cich, M. J., Rowen, A. M., Arrington, C. L., Lee, M., Grine, A. D., Fuller, C. T., Reno, J. L., and Young, E. W., "Terahertz quantum cascade laser integration with on-chip micromachined rectangular waveguides," Terahertz Technology and Applications II **7215**(1), 721504 (2009).

[15] Amanti, M. I., Fischer, M., Walther, C., Scalari, G., and Faist, J., "Horn antennas for terahertz quantum cascade lasers," Electron Lett **43**, 573–574 (Jan 2007).

[16] Rowen, A., Hollowell, A. E., Wanke, M. C., Nordquist, C. D., Arrington, C. L., Gillen, J. R., and Coleman, J. J., "Multi-layer metal micromachining for thz waveguide fabrication," Micromachining and Microfabrication Process Technology XV **7590**, 759009 (Feb 2010).

[17] Nordquist, C. D., Wanke, M. C., Rowen, A. M., Arrington, C. L., Grine, A. D., and Fuller, C. T., "Properties of surface metal micromachined rectangular waveguide operating near 3 thz," Selected Topics in Quantum Electronics, IEEE Journal of **17**(1), 130 – 137 (2011).

[18] Digby, J., McIntosh, C., Parkhurst, G., Towlson, B., Hadjiloucas, S., Bowen, J., Chamberlain, J., Pollard, R., Miles, R., Steenson, D., Karatzas, L., Cronin, N., and Davies, S., "Fabrication and characterization of micromachined rectangular waveguide components for use at millimeter-wave and terahertz frequencies," Ieee T Microw Theory **48**, 1293–1302 (Jan 2000).

[19] Kirby, P., Pukala, D., Manohara, H., Mehdi, I., and Papapolymerou, J., "Characterization of micromachined silicon rectangular waveguide at 400 ghz," IEEE MICROWAVE AND WIRELESS COMPONENTS LETTERS **16**, 366–368 (Jan 2006).

[20] Adam, A., Kašalynas, I., Hovenier, J., Klaassen, T., Gao, J., Orlova, E., Williams, B., Kumar, S., Hu, Q., and Reno, J., "Beam patterns of terahertz quantum cascade lasers with subwavelength cavity dimensions," Appl Phys Lett **88**, 151105 (2006).

[21] Orlova, E., Hovenier, J., Klaassen, T., Kasalynas, I., Adam, A., Gao, J., and Klapwijk, T., "Antenna model for wire lasers," Phys Rev Lett **96**, 173904 (Jan 2006).

[22] Lee, A. W. M., Qin, Q., Kumar, S., Williams, B. S., Hu, Q., and Reno, J. L., "High-power and high-temperature thz quantum-cascade lasers based on lens-coupled metal-metal waveguides," Opt Lett **32**, 2840–2842 (Jan 2007).

[23] Wanke, M., Lee, M., and Nordquist..., C., "Monolithically integrated thz transceivers," Novel In-Plane Semiconductor Lasers X **7953**, 79530S–1 (Jan 2011).

[24] Jukam, N., Dhillon, S. S., Oustinov, D., Madeo, J., Manquest, C., Barbieri, S., Sirtori, C., Khanna, S. P., Linfield, E. H., Davies, A. G., and Tignon, J., "Terahertz amplifier based on gain switching in a quantum cascade laser," Nat Photonics **3**, 715–719 (Jan 2009).

[25] Wanke, M. C., Young, E. W., Nordquist, C. D., Cich, M. J., Grine, A. D., Fuller, C. T., Reno, J. L., and Lee, M., "Monolithically integrated solid-state terahertz transceivers," Nat Photonics **4**, 565–569 (Jan 2010).